

Numerical modeling of residual stress induced by laser shock processing



X.L. Wei^{a,b}, X. Ling^{a,b,*}

^a Jiangsu Key Laboratory of Process Enhancement and New Energy Equipment Technology, Nanjing 210009, China

^b School of Mechanical and Power Engineering, Nanjing University of Technology, Nanjing 210009, China

ARTICLE INFO

Article history:

Received 29 October 2013

Received in revised form

25 December 2013

Accepted 21 February 2014

Available online 1 March 2014

Keywords:

Laser shock processing

Finite element simulation

Residual stress

35CD4 30HRC steel

ABSTRACT

Laser shock processing (LSP) is proving to be a competitive technology to traditional surface enhancement techniques in engineering products. The LSP develops a significant residual compressive stress deep into the surface of a metal alloy, which is beneficial for fatigue, wear and corrosion. In this paper, a comprehensive three-dimensional model is presented to predict the development, magnitude and distribution of residual stress field induced by LSP. In order to verify the FEA model, a benchmark simulation is performed verified with available experimental results. The predicted residual stress field for single laser shock processing is well correlated with experimental data. With the aid of the model, the influences of LSP parameters such as full width at half maximum (FWHM), power density, spot size, number of shots and overlapped shots have been analyzed. Some optimized parameters of LSP can be made by employing the presented models and results of the parametric investigations.

© 2014 Elsevier B.V. All rights reserved.

1. Introduction

White [1] used high-energy pulsed lasers to generate shock waves and plastic deformation in metallic targets for the first time, with the development of confined ablation modes extended by Anderholm [2]. Laser shock processing emerges to be a competitive technology as a method of imparting compressive residual stresses into the surface of metals to improve fatigue life and corrosion resistance in the past several decades. Compared with the traditional surface enhancement techniques such as shot peening, the advantages of LSP include high magnitude of compressive residual stress, deeper plastic deformation layer, increased control in application and reduced microstructural damage [3].

Many investigations have concentrated on experimentally determining mechanical effects including residual stress field and surface morphology significantly enhancing the fatigue life and corrosion resistance abilities of metals [4–10]. During a LSP process, it is very difficult to monitor and investigate the dynamic responding process as well as residual stress in the target by means of experimental approaches. In addition, it is not enough using an analytical model to describe the complex process. In this case, the

finite element analysis (FEA) method can be applied to simulate the LSP process for the further exploration and development of the LSP process of materials. Braisted and Brockman [11] used finite element analysis techniques to predict the residual stress induced by laser shock processing. Arif [12] investigated a finite difference algorithm to simulate propagation of stress wave in the material. Ding and Ye [13] applied 2-D simulation to predict the development, magnitude and distribution of residual stress, however, only a single LSP treatment and multiple LSP treatments were discussed. Hu et al. [14] developed a 3-D simulation and only a single and multiple laser shocks were performed. Peyre et al. [15] presented a 2-D FEA model to calculate the residual stresses and performed parametric investigations for a single LSP shot. Warren et al. [16] investigated the effects of parallel multiple laser-material interaction on the stress and strain distributions during LSP. Wu et al. [17] developed a physics-based model for femtosecond laser pulses and performed a single LSP treatment and multiple LSP treatments simulation. Achintha and Nowell [18] presented an eigenstrain model of the residual stresses to investigate the effects of work dimensions and multiple shots. Singh et al. [19,20] performed the optimization investigation for multiple laser peening process by modified particle swarm optimization. Singh et al. [21] used elliptical laser spot shapes to perform parametric investigations for a LSP process. These investigations are limited to two or three settings of LSP parameters: power density or peak pressure, spot size and number of shots. With the increasing wide application of LSP industry, more complicated cases including parameters such as

* Corresponding author at: School of Mechanical and Power Engineering, Nanjing University of Technology, Nanjing 210009, China. Tel.: +86 25 83243112; fax: +86 25 83600956.

E-mail address: Xling@njtech.edu.cn (X. Ling).

laser spot shape, FWHM and overlapped shots need to be put forward.

In this paper, a three-dimensional model is presented to predict the development, magnitude and distribution of residual stress field induced by LSP. Benchmark simulation for a single LSP is performed and validated, in which laser spot shape is square in order to avoid concentration of release waves at the center. Once the process is validated, the influences of LSP parameters such as FWHM, power density, spot size, number of shots and overlapped shots are discussed.

2. Finite element modeling

2.1. Loading

In the confined ablation mode, the laser energy is deposited through the transparent overlay to the interface between the target and the transparent overlay. As the volume of the plasma is heated and vaporized by the laser pulse, the volume of the plasma is expected to expand at the interface. The expanding plasma produces the propagation of the induced shock waves into both the confined overlay and target. In this case, the peak pressure P is given by Fabbro et al. [22]:

$$P(\text{GPa}) = 0.01 \sqrt{\frac{\alpha}{2\alpha + 3}} \sqrt{Z(\text{g cm}^{-2} \text{s}^{-1})} \sqrt{I_0(\text{GW cm}^{-2})} \quad (1)$$

where I_0 is the incident laser power density; P is the pressure; Z is the reduced shock impedance between the target and the confining materials; α is the efficiency of the interaction, where α is devoted to the pressure increase of the plasma ($\alpha = 0.1\text{--}0.2$) [22]. Especially, when a confined ablation mode with water overlay is applied in LSP process, Eq. (1) could be simplified as [22]:

$$P(\text{GPa}) = 1.02 \sqrt{I_0(\text{GW cm}^{-2})} \quad (2)$$

Berthe et al. [23] performed significant experimental efforts to determine the pressure–time history and spatial distribution of the loading. Zhang and Yao [24] developed the spatially nonuniform shock pressure as normal distribution. Amarchinta et al. [25] developed an experiment-based pressure load model, which has both time and spatial variation. Generally, the pressure–time history is modeled as a triangular ramp in the simulation, in which the pressure rises linearly to the peak pressure over the time of the pressure pulse FWHM and decays linearly to zero within the following FWHM [14,18]. The spatial distribution of the loading is extremely difficult to investigate experimentally and has been widely assumed that the pressure develops uniformly over the area covered by laser pulse.

2.2. Constitutive model

LSP generates strain-rates exceeding 10^6 s^{-1} within the workpiece material. At such high rates, metals behave significantly different from that under quasi-static conditions. With the increase of the strain-rate, metals typically present little change in elastic modulus and an increase in yield strength. As the strain-rate increases, the response becomes a shock wave phenomenon. Amarchinta et al. [25,26] performed a great deal of research on material model for LSP simulation. Simply, elastic-plastic material model is used here. The elastic limit stress in the direction of the shock wave propagation is defined as the Hugoniot Elastic Limit (HEL) [11]. When the peak pressure is greater than the HEL, the plastic strain occurs. If it is assumed that the yielding occurs when the stress in the direction of the wave propagation reaches the HEL,

Table 1
Chemical composition of 35CD4 steel.

C	Mn	Si	S	P	Ni	Cr	Mo
0.37	0.79	0.30	0.010	0.019	<0.17	1.00	0.18

Table 2
Mechanical properties of 35CD4 30HRC steel.

Material property	Value	Unit
Density (ρ)	7800	kg m^{-3}
Poisson's ratio (ν)	0.29	
Elastic modulus (E)	210	GPa
Hugoniot elastic limit (HEL)	1.47	GPa
Water impedance (Z_2)	1.65×10^5	$\text{g cm}^{-2} \text{ s}^{-1}$
Acoustic impedance (Z_1)	3.6×10^6	$\text{g cm}^{-2} \text{ s}^{-1}$

then the dynamic yield strength under uniaxial stress conditions can be defined in terms of the HEL by Braisted and Brockman [11]:

$$\sigma_{dyn} = \text{HEL} \frac{1 - 2\nu}{1 - \nu} \quad (3)$$

where ν is the Poisson's ratio. It is assumed that the workpiece material is homogeneous and isotropic, and also is perfectly elastic-plastic with the dynamic yield strength defined in Eq. (3). The material is 35CD4 30HRC steel shown in Tables 1 and 2.

2.3. Geometric modeling

A three-dimensional finite element analysis model has been developed to perform benchmark simulation and investigate residual stress field of 35CD4 30HRC steel treated by LSP. Since the model is symmetric and subjected to a symmetric uniform pressure pulse load, a quarter of the configuration of this model with size $10 \text{ mm} \times 10 \text{ mm} \times 10 \text{ mm}$ is considered to perform the finite element calculation considering computational efficiency, as shown in Fig. 1, in which a fine mesh consists of $5 \text{ mm} \times 5 \text{ mm} \times 5 \text{ mm}$ elements.

2.4. Simulation procedure

The finite element codes, ABAQUS/Explicit and ABAQUS/Standard have been used to complete these simulations, which could be described in two major steps. The first step is that the pressure induced by laser beam and other necessary parameters are guided into ABAQUS/Explicit for dynamic response of the target, and an ABAQUS/Explicit analysis is performed until all the plastic deformation has occurred. In ABAQUS/Explicit, the dissipated energy during dynamic response is monitored,

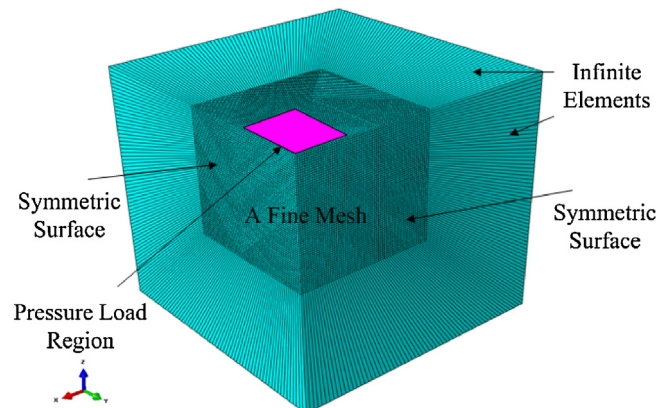


Fig. 1. Schematic configuration of 3-D model.

Download English Version:

<https://daneshyari.com/en/article/5350879>

Download Persian Version:

<https://daneshyari.com/article/5350879>

[Daneshyari.com](https://daneshyari.com)